Guo et al. *Quantum Frontiers* (2025) 4:23
https://doi.org/10.1007/s44214-025-00096-2

Quantum Frontiers

ORIGINAL ARTICLE Open Access

Benchmark quantum computer with analytical single spin-flip dynamics

Zheng-Xin Guo[1†], Xi-Dan Hu[2,3†], Qi-Qi Su[4], Xue-Jia Yu[5*] and Zhi Li[2,3*]

Abstract

The physical world is inherently out of equilibrium, and understanding the non-equilibrium behavior of quantum many-body systems remains a key open challenge in condensed matter physics. Recent advances in quantum computing platforms, such as Rydberg atoms and superconducting qubits, have opened promising avenues for studying non-equilibrium dynamics of many-particle systems using quantum simulators. In this work, we propose a benchmark scheme for validating the dynamical evolution outcomes of future large-scale qubit systems, which far exceeds the capability of classical numerical benchmark. Based on the $J_1 - J_2$ Heisenberg model, we provide tunable analytical results including quantum walk dynamics, the out-of-time-ordered correlator (OTOC), and the butterfly velocity. Furthermore, taking IBM's programmable quantum platform as an example, we design a scheme for simulating quantum walk dynamics and experimentally demonstrate the feasibility of benchmarking with our proposed dynamical observables.

Keywords: Quantum computation, Benchmark, Quantum walk, Out-of-time-ordered correlator

1 Introduction

The study of non-equilibrium phenomena in quantum many-body systems remains a central frontier of condensed matter physics [1–3]. Recent programmable quantum computer utilizing Rydberg-atom, trapped ions and superconducting circuit platforms incorporating hundreds of qubits, opens a direct path to simulating quantum many-body dynamics on an unprecedented scale [4–8]. As these devices continue to grow in size and complexity, the pressing need arises for corresponding theoretical protocols and benchmarking methodologies to validate the outcomes of such dynamical simulations.

As one of the few tunable dynamical processes in such systems, quantum walks (QW) offer promising prospects for technological applications in quantum computing and related areas [9–16]. The pioneering work by Childs *et al.* in 2009 established that continuous-time QW can serve as a universal computational model for programmable quantum computers [11, 12], sparking extensive research in subsequent years. To date, QW has been experimentally demonstrated across a wide range of simulation platforms, including optical systems [17–30], trapped ions [31–35], ultracold atomic gases [36–42], and superconducting circuits [43–46], among others.

On another front, the transport properties of quantum many-body systems are intimately connected to the speed at which quantum information propagates. This has motivated growing attention to out-of-time-ordered correlators (OTOCs) as key indicators of thermalization and information scrambling [47–52]. Serving as a quantum generalization of the classical Poisson bracket, OTOCs capture the growth of non-commutativity between operators over time. They have been widely employed to characterize information spreading in diverse settings, including

*Correspondence: xuejiayu@fzu.edu.cn; lizphys@m.scnu.edu.cn
[5]Fujian Key Laboratory of Quantum Information and Quantum Optics, College of Physics and Information Engineering, Fuzhou University, Fuzhou, Fujian, 350108, China
[2]Key Laboratory of Atomic and Subatomic Structure and Quantum Control (Ministry of Education), Guangdong Basic Research Center of Excellence for Structure and Fundamental Interactions of Matter, School of Physics, South China Normal University, Guangzhou, 510006, China
Full list of author information is available at the end of the article
†Equal contributors

quantum many-body dynamics [53–61], many-body localized phases [62–71], quantum chaotic systems [72–77], and even holographic black hole models [78–81]. Notably, Maldacena, Shenker, and Stanford provided the first theoretical proof of a fundamental bound, the exponential growth limit, on operator growth in black hole physics and the SYK model [79], thereby reinforcing the AdS/CFT correspondence [80, 81]. Experimentally, OTOCs have been measured in several table-top quantum simulators [59, 60, 62, 82–89], establishing them as essential observables for studying information dynamics.

In this work, we present an analytical scheme based on the $J_1 - J_2$ Heisenberg model and linear spin-wave theory. We demonstrate that the dynamics of a single-spin-flip QW, the OTOCs, and the butterfly velocity can be accurately and efficiently characterized within this scheme. Owing to its computational efficiency and tunability, our scheme provides a practical approach for benchmarking non-equilibrium dynamics on future large-scale quantum processors. The dynamical results of our scheme are verified by multiple numerical approaches at various scales. Furthermore, we implement a proof-of-principle experiment on an IBM programmable quantum computer, confirming that the non-equilibrium observables derived from our theory are directly measurable on current quantum devices.

2 Visualized QW

2.1 Spin wave thoery

The model adopted in this letter is a square-lattice ferromagnetic J_1-J_2 Heisenberg model, and the related Hamiltonian can be written as

$$\begin{aligned}\hat{H} =& J_1 \sum_{m,n} (\hat{\mathbf{S}}_{m,n}\hat{\mathbf{S}}_{m\pm1,n} + \hat{\mathbf{S}}_{m,n}\hat{\mathbf{S}}_{m,n\pm1}) \\ &+ J_2 \sum_{m,n} \hat{\mathbf{S}}_{m,n}\hat{\mathbf{S}}_{m\pm1,n\pm1},\end{aligned} \tag{1}$$

where J_1 and J_2 correspond to the nearest-neighboring (nn) and the next-nearest-neighboring (nnn) spin exchange coupling, respectively. For simplicity, we consider only the ferromagnetic case, i.e., $J_1 < 0$ and $J_2 < 0$.

Based on the linear spin wave (SW) theory, one can exactly diagonalize the Hamiltonian of the system (see supplementary materials [90] for details). By performing Holstein-Primakoff transformation and Fourier transformation for Eq. (1), Hamiltonian of the magnon can be obtained as

$$\begin{aligned}\hat{\tilde{H}} =& \sum_{\mathbf{k}} \omega_{\mathbf{k}} \hat{a}^\dagger_{\mathbf{k}} \hat{a}_{\mathbf{k}} + J_1 \sum_{i,j} (\hat{n}_{i,j}\hat{n}_{i\pm1,j} + \hat{n}_{i,j}\hat{n}_{i,j\pm1}) \\ &+ J_2 \sum_{i,j} (\hat{n}_{i,j}\hat{n}_{i\pm1,j\pm1}),\end{aligned} \tag{2}$$

where $\hat{n}_{i,j}$ is the particle number operator and the second(third) term represents two-body interaction between nn(nnn) sites. $\omega_{\mathbf{k}}$ stands for the energy of magnons, which has the following expressions,

$$\omega_{\mathbf{k}} = 2[J_1(1 - \gamma_{1\mathbf{k}}) + J_2(1 - \gamma_{2\mathbf{k}})], \tag{3}$$

$$\gamma_{1\mathbf{k}} = \frac{1}{2}(\cos k_x + \cos k_y), \tag{4}$$

$$\gamma_{2\mathbf{k}} = \frac{1}{2}[\cos(k_x + k_y) + \cos(k_x - k_y)]. \tag{5}$$

2.2 Spin-flip dynamics and magnon's QW

Then, one can readily study the propagation behavior of magnons with the diagonalized Hamiltonian, and figure out how the single spin flip information diffuses in the background of the ferromagnetic ground state. Let's start with calculating the density distribution versus time, which is a key observable easy to measure experimentally in studying QW, with its expression as [37–39],

$$\xi(\mathbf{r}, t) = \langle\phi|\hat{S}^+_{\mathbf{r}_0}\hat{S}^z_{\mathbf{r}_{m,n}}(t)\hat{S}^-_{\mathbf{r}_0}|\phi\rangle, \tag{6}$$

with

$$\hat{S}^z_{\mathbf{r}_{m,n}}(t) = e^{iHt/\hbar}\hat{S}^z_{\mathbf{r}_{m,n}}e^{-iHt/\hbar}, \tag{7}$$

where $|\phi\rangle$ is the initial state, i.e., the ferromagnetic ground state and $\mathbf{r} = \mathbf{r}_{m,n} - \mathbf{r}_0$. In the expression, $\hat{S}^z_{\mathbf{r}_{m,n}}$ represents the spin operator at $\mathbf{r}_{m,n}$ in z-direction, while $\hat{S}^+_{\mathbf{r}_0}$ and $\hat{S}^-_{\mathbf{r}_0}$ denote the spin flip up and down operators at $\mathbf{r}_0$, respectively. The diffusion behavior of the magnon can be revealed by measuring the evolution of density distribution with time.

Since this is a ferromagnetic (FM) system, the single spin-flip on top of the fully polarized FM ground state can be exactly mapped to a single hard-core boson in the vacuum state. As is known to all, in FM case, the Hamiltonian ignoring the interacting terms is still exact for single-magnon sectors. Hence, we can substitute the effective Hamiltonian

$$\hat{H}_{eff} = \sum_{\mathbf{k}} \omega_{\mathbf{k}} \hat{a}^\dagger_{\mathbf{k}} \hat{a}_{\mathbf{k}} \tag{8}$$

into Eq. (6). Considering the operation rules of creation and annihilation operators, one can obtain the analytical expression of QW((see supplementary material [90] for details), i.e.,

$$\xi(\mathbf{r}, t) = \left| \sum_{\mathbf{k}} \frac{e^{-i(\mathbf{k}\cdot\mathbf{r} + \omega_{\mathbf{k}}t/\hbar)}}{N^2} \right|^2. \tag{9}$$

Thus, we can obtain the exact solution of the time-evolution that involves a great number of qubits on two-dimensional computing platform.

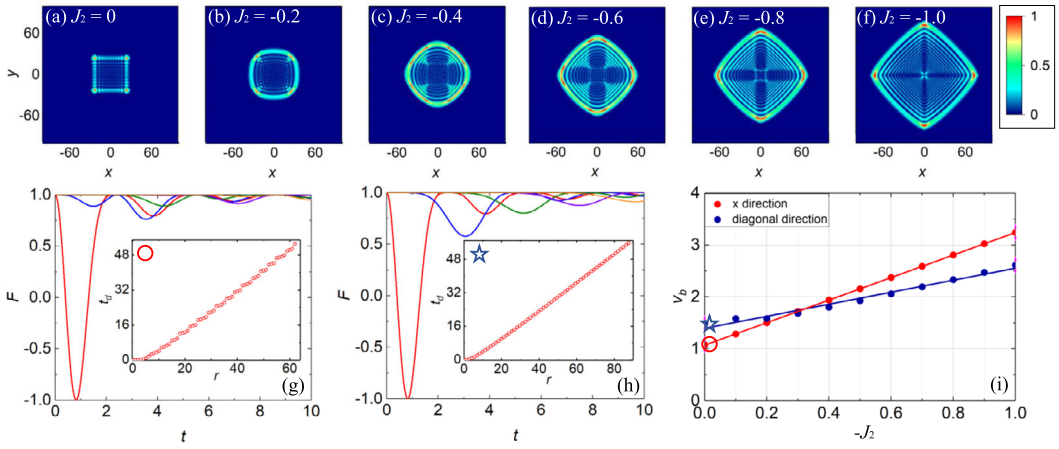

Figure 1 (Color online). Visualized magnon QW and spread properties of ferromagnetic J_1-J_2 Heisenberg model with nn and nnn interaction. (a-f) The density distributions of magnon with different nnn interaction strengths J_2 at $t = 25$. (g) The OTOC along x direction for different distance $|\mathbf{r}| = \mathbf{r}_{m,0} - \mathbf{r}_0 = 0$ (red), 2 (blue), 4(green), 6(purple), 8 (orange). (h) The OTOC along diagonal direction for different $|\mathbf{r}| = \mathbf{r}_{m,n=m} - \mathbf{r}_0 = 0$ (red), $2\sqrt{2}$ (blue), $4\sqrt{2}$ (green), $6\sqrt{2}$ (purple), $8\sqrt{2}$ (orange). Insets: The t_d lines (line of first decline moments) for x-axis and diagonal. (i) Butterfly velocities for different nnn interaction. Throughout, $J_1 = -1$. The unit of x and y is the lattice constant a = 1, whereas the time unit here is $\hbar/|J_1| = 1$ with $\hbar = 1$

For convenience, we refer to the above technique as analytical single spin-flip dynamics (ASSD). The process of magnon's dynamic evolution under different parameters J_2 is visualized in Figs. 1(a-f). As shown in the figure, when $J_2 = 0$, the system degenerates to the standard Heisenberg model. The density distribution then features ballistic propagation, typical for QW. When $J_2 \neq 0$, the nnn coupling comes into play. As shown in Fig. 1, the influence of the nnn coupling on dynamics of the system can be distilled into three points:

I. J_2 causes the magnon to travel faster in all directions. As we know, the computation speed of quantum computers is closely related to the speed of information propagation between qubits. The observed acceleration of information propagation is connected to the computational speedups in quantum algorithms such as spatial search based on quantum walks [91].

II. The acceleration is anisotropic, maximum in the x- and y-axis directions and minimum in the diagonal direction. Therefore, new quantum computers can be designed on the basis of the anisotropic propagation, which will play a pivotal role in conducting anisotropic computation and quantum simulation effectively.

III. The competition between nn and nnn coupling cannot destroy the ballistic propagation behavior. However, the geometric structure of ballistic propagation can be changed by manipulating parameters J_1 and J_2. As shown in Figs. 1(a-f), the system transforms from a square structure to a rhombic QW.

3 OTOCs and butterfly velocities

Furthermore, we calculate OTOCs of the system and the corresponding butterfly velocity to reveal the propagation characteristics [53–60, 82–85]. Note that butterfly velocity and the Lieb-Robinson bounds (the upper limit of the information propagation speed in quantum systems) are highly interdependent, which reflects information propagation behavior in many-body systems [47, 92–98]. Detailed derivation of OTOCs and butterfly velocity in J_1-J_2 model is included in Supplementary Material [90].

By simple operator gymnastics, one can obtain the analytic expression of the system's OTOCs, which reads

$$\hat{F}(t) = \langle\phi|\hat{S}^+_{\mathbf{r}_0}\hat{S}^z_{\mathbf{r}_{m,n}}(t)\hat{S}^z_{\mathbf{r}_0}(0)\hat{S}^z_{\mathbf{r}_{m,n}}(t)\hat{S}^z_{\mathbf{r}_0}(0)\hat{S}^-_{\mathbf{r}_0}|\phi\rangle. \tag{10}$$

Then, we get OTOCs' analytical expression as

$$\hat{F}(t) = 1 - 8/N^2\Omega_1\Omega_2 + 8/N^4\Omega_1\Omega_2\Omega_1\Omega_2, \tag{11}$$

where,

$$\begin{aligned}\Omega_1 &= \sum_{\mathbf{k}} e^{-i\mathbf{k}\cdot(\mathbf{r}_0-\mathbf{r}_{m,n})}e^{i\omega_{\mathbf{k}}t/\hbar},\\ \Omega_2 &= \sum_{\mathbf{k}} e^{i\mathbf{k}\cdot(\mathbf{r}_0-\mathbf{r}_{m,n})}e^{-i\omega_{\mathbf{k}}t/\hbar}.\end{aligned} \tag{12}$$

Based on the ASSD technique, the propagation properties of magnetic information (a spin-flip signal) in the large-scale J_1-J_2 Heisenberg model can be revealed at a lower computational cost.

The results of OTOCs and the butterfly velocity are plotted in Figs. 1(g-i). We define the time when OTOC begins to decline as the critical time t_d. The illustration reflects the relationship between t_d and $\mathbf{r}$. As shown in Fig. 1(g) [(h)], the OTOCs along the x-, y-axis [diagonal] direction

oscillate versus time, where the amplitude of OTOCs decreases and t_d increases with the increasing $\mathbf{r}$. Since the magnon wave packet itself is conservative in the process of evolution, the probability of magnon distribution at a distant point is relatively small, hence the relatively small amplitude [47–49]. Besides, the propagation mode of the system is determined by the growth of the local Heisenberg operator, therefore, the longer the propagation time of the distant lattice magnon, the larger the corresponding t_d. The above two points well reflect that the magnon information diffuses in a way of QW. Note that the slope of t_d in the illustration is the butterfly velocity [72, 73]. Further, we calculate how the butterfly velocity of the system changes with J_2 [see Fig. 1(i)]. As shown in the figure, when J_2 increases, the butterfly velocity in the diagonal direction will slowly surpass that in the x-direction, which indicates that the butterfly velocity can very well reflect the competitive relationship between nn coupling and nnn coupling in the system.

In short, based on OTOCs and butterfly velocity, one can understand the features of magnon QW in J_1-J_2 model from the following three perspectives:

I. The superposition of another QW on top of the previous one will lead to the acceleration of information propagation;

II. The competition between the two results in the change from diagonal dominance to x- and y-axis dominance of QW, and correspondingly, the geometric structure changes from square to rhombus;

III. The introduction of nnn coupling will not destroy the ballistic propagation mode, therefore, the system still displays QW.

It is noticeable that the QW and OTOCs results of a single spin-flip are totally accurate, which is supported by mathematical proofs in the previous sections and double-checked by Exact Diagonalization and TDVP in the Supplementary Material [90].

4 Digital quantum simulation

In principle, SW theory can very effectively describe the diffusion process of information in large-scale or even infinite lattice ferromagnetic systems, thus making it an ideal way to test the computational power of quantum computers. We believe that the coming decades will see a great increase in the number of qubits, as well as the realization of error-correcting qubits. With the unstoppable progress of technological infrastructure, more phenomena in many-body dynamics, such as QW in large-scale systems and controllable magnetic transport, will be verified by more programmable quantum processors in the future.

As a principle testing, here we conduct experiments on a 5-qubit quantum processor and compare the experimental results with the theoretical ones. In order to conduct an experiment of scrambling dynamics on the IBM quantum processor, one must translate the time evolution into the language of quantum circuits, i.e., a series of standard quantum gates. First, the Heisenberg model described in boson language can be written as

$$H = -\frac{1}{2}N + 2\sum_l(\hat{a}_l^\dagger \hat{a}_l) - \sum_l(\hat{a}_l\hat{a}_{l+1}^\dagger + \hat{a}_l^\dagger \hat{a}_{l+1}). \tag{13}$$

Here we take $J_1 = -1$ and $S = 1/2$. By ignoring the constant term, which only brings in a global phase factor, the time evolution operator can be written as

$$\hat{U}(\delta t) = e^{-iH\delta t} = e^{-i[2\sum_l(\hat{a}_l^\dagger \hat{a}_l) - \sum_l(\hat{a}_l\hat{a}_{l+1}^\dagger + \hat{a}_l^\dagger \hat{a}_{l+1})]\delta t}. \tag{14}$$

For tiny δt, the Trotter decomposition can be used to break the evolutionary operator into the following steps,

$$\begin{aligned}\hat{U}(\delta t) &\simeq e^{-i\sum_l(\hat{a}_l^\dagger \hat{a}_l)\delta t} e^{i\sum_l(\hat{a}_l\hat{a}_{l+1}^\dagger + \hat{a}_l^\dagger \hat{a}_{l+1})\delta t} e^{-i\sum_l(\hat{a}_l^\dagger \hat{a}_l)\delta t} \\ &= \hat{U}_1(\delta t)\hat{U}_2(\delta t)\hat{U}_1(\delta t).\end{aligned} \tag{15}$$

where $\hat{U}_1$ and $\hat{U}_2$ represent the contribution of the on-site term and nn term. Next, we need to implement the $\hat{U}_1$ and $\hat{U}_2$ operators with a series of single and double qubit logic gates. $\hat{U}_1$ can be readily implemented via a single qubit logic gate, while $\hat{U}_2$ can be formed by the combination of C-NOT gate, Y gate and Z gate, as shown in Fig. 2(a). The input parameter θ is a function of δt and J_1. In the experiment, $\delta t = 0.1$ and $J_1 = -1$. Thus, a complete life cycle of time-evolving operation can be written as the quantum circuit in Fig. 2(b).

Figure 2(c) shows the magnon dynamic evolution behavior obtained via four different methods (analytical solution of SW theory, exact diagonalization method, IBM simulator and real IBM quantum processor). The results obtained by all these methods are consistent, i.e., the system exhibits the feature of QW. It is worth noting that the analytical solution calculated by SW stands out as the ideal choice, for it can predict the dynamic evolution behavior of large-scale magnetic models at a lower computational cost of classical computers.

Since the analytical solution given here has universality, it can be used as a "standard" to measure the performance and fidelity of large-scale quantum chips in the future. Currently, since quantum computers are limited in fidelity and number of qubits, only small-scale models can be simulated. Recent experiments with quantum circuits, however, have shown more and more controllable qubits [45, 46]. In the future, with the increase of the number of qubits and the advent of error-correcting qubits, more phenomena of many-body dynamics can be studied using the method presented in this paper.

It is important to discuss the restriction of our ASSD scheme to systems with spatial translational symmetry.

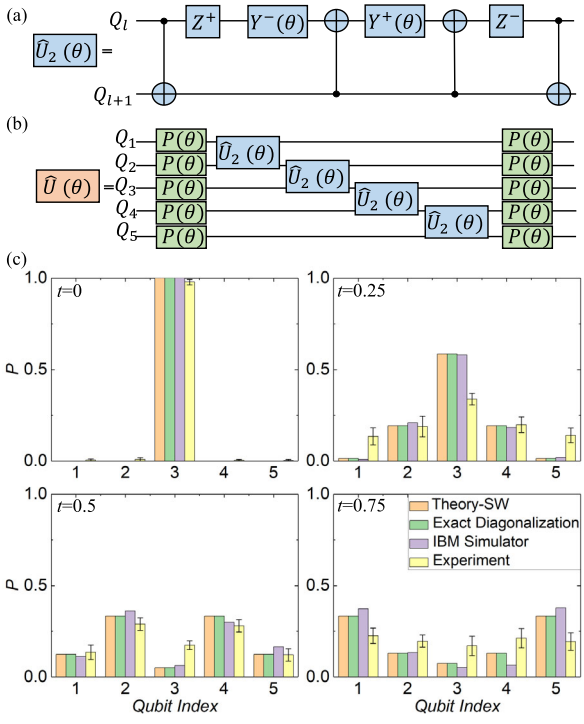

Figure 2 (Color online). The illustration of quantum circuit. (a) The quantum circuit of two-qubit time-evolution operation, where $Z^{\pm} = e^{\mp i(3\pi/2)\sigma_z}$ and $Y^{\pm} = e^{\mp i(\theta/2)\sigma_y} = e^{\mp i(\delta t/2)\sigma_y}$. (b) The quantum circuit which realizes the complete time-evolution operation, where $P(\theta)$ is the standard phase transition gate and $\theta = \delta t$. (c) The single spin-flip dynamics of theoretical and experimental approaches when $t = 0$, $t = 0.25$, $t = 0.5$, and $t = 0.75$, respectively

This focus, however, is a deliberate strength for a benchmark. Systems without such symmetry are inherently challenging for fidelity benchmarking, as the necessary average over disorder realizations obscures the intrinsic error profile of the quantum hardware. The central aim of our work is to identify a sweet spot that balances benchmarking accuracy with the simulation of large-scale quantum dynamics. By utilizing translationally symmetric systems, we achieve a clear, unambiguous measure of device performance.

5 Conclusion

As the accuracy and the number of entangled qubits continuously increase, numerical methods will start to lose their reliability due to the ascending calculation cost and error when solving non-equilibrium problems. Thus, effective techniques that can verify the capability of quantum computers that involve a large number of qubits are needed. In this connection, we propose a technique from the perspective of dynamics. By conducting a single spin-flip on top of the ground state of a two-dimentional ferromagnetic J_1-J_2 Heisenberg model and simulating the time-evolution of QW and OTOCs with an analytical procedure, we can provide large-scale quantum computer with a decent benchmark. Moreover, the accuracy and superiority of the analytical procedure overtake those of the numerical methods of TDVP and ED. Finally, we prove an experiment on IBMQ to justify the selection of dynamical observable, and look forward to seeing future realization of this scheme on larger-scale quantum computation platforms. Our work will provide quantum computation researchers with a useful tool and shed light on quantum information, quantum chaos and traditional condensed matter physics.

Author contributions

Z-XG and X-DH did the theoretical and numerical work with the input from ZL and X-JY. All authors participated in the analysis of the results. ZL and X-JY provided the original idea. Z-XG wrote the manuscript with the input from all authors. Q-QS wrote the quantum computing part of the supplementary material. All authors have read and approved the manuscript.

Funding information

This work was supported by the National Key Research and Development Program of China (Grant No. 2022YFA1405300), Guangdong Provincial Quantum Science Strategic Initiative (Grant No. GDZX2204003), Innovation Program for Quantum Science and Technology (Grant No. 2021ZD0301700), the Guangdong Basic and Applied Basic Research Foundation (Grant No. 2021A1515012350), Guangdong Provincial Quantum Science Strategic Initiative (Grants No. GDZX2304002 and GDZX2404001), the Open Fund of Key Laboratory of Atomic and Subatomic Structure and Quantum Control (Ministry of Education), and the National Natural Science Foundation of China (Grant No. 12405034).

Data availability

All data underlying the results are available from the authors upon reasonable request.

Declarations

Competing interests

The authors declare no competing interests.

Author details

[1]Wilczek Quantum Center and Key Laboratory of Artificial Structures and Quantum Control, School of Physics and Astronomy, Shanghai Jiao Tong University, Shanghai, 200240, China. [2]Key Laboratory of Atomic and Subatomic Structure and Quantum Control (Ministry of Education), Guangdong Basic Research Center of Excellence for Structure and Fundamental Interactions of Matter, School of Physics, South China Normal University, Guangzhou, 510006, China. [3]Guangdong Provincial Key Laboratory of Quantum Engineering and Quantum Materials, Guangdong-Hong Kong Joint Laboratory of Quantum Matter, Frontier Research Institute for Physics, South China Normal University, Guangzhou, 510006, China. [4]Guangzhou Tianhe Foreign Language School, Guangzhou, 510627, China. [5]Fujian Key Laboratory of Quantum Information and Quantum Optics, College of Physics and Information Engineering, Fuzhou University, Fuzhou, Fujian, 350108, China.

Received: 13 October 2025 Revised: 25 November 2025
Accepted: 7 December 2025 Published online: 19 December 2025

References

1. A. Zagoskin, *Quantum Theory of Many-Body Systems: Techniques and Applications* (Springer, Berlin, 2014)
2. I. Bloch, J. Dalibard, W. Zwerger, Many-body physics with ultracold gases. Rev. Mod. Phys. **80**, 885 (2008)
3. L. Amico, R. Fazio, A. Osterloh, V. Vedral, Entanglement in many-body systems. Rev. Mod. Phys. **80**, 517 (2008)

4. S. Ebadi, T.T. Wang, H. Levine, et al., Quantum phases of matter on a 256-atom programmable quantum simulator. Nature **595**, 227–232 (2021)
5. P. Scholl, M. Schuler, H.J. Williams, et al., Quantum simulation of 2D antiferromagnets with hundreds of Rydberg atoms. Nature **595**, 233–238 (2021)
6. S.-A. Guo, Y.-K. Wu, J. Ye, et al., A site-resolved two-dimensional quantum simulator with hundreds of trapped ions. Nature **630**, 613–618 (2024)
7. J.M. Martinis, M.H. Devoret, J. Clarke, Energy-level quantization in the zero-voltage state of a current-biased Josephson junction. Phys. Rev. Lett. **55**, 1543 (1985)
8. S.-Z. Li, et al., Multifractal-enriched mobility edges and emergent quantum phases in Rydberg atomic arrays. Sci. China, Phys. Mech. Astron. **69**, 217212 (2026)
9. Y. Aharonov, L. Davidovich, N. Zagury, Quantum random walks. Phys. Rev. A **48**, 1687 (1993)
10. N. Shenvi, J. Kempe, K.B. Whaley, Quantum random-walk search algorithm. Phys. Rev. A **67**, 052307 (2003)
11. A.M. Childs, Universal computation by quantum walk. Phys. Rev. Lett. **102**, 180501 (2009)
12. A.M. Childs, D. Gosset, Z. Webb, Universal computation by multiparticle quantum walk. Science **339**, 791 (2013)
13. S. Chakraborty, K. Luh, J. Roland, How fast do quantum walks mix? Phys. Rev. Lett. **124**, 050501 (2020)
14. L.K. Upreti, C. Evain, S. Randoux, P. Suret, A. Amo, P. Delplace, Topological swing of Bloch oscillations in quantum walks. Phys. Rev. Lett. **125**, 186804 (2020)
15. P. Wrzosek, K. Wohlfeld, D. Hofmann, T. Sowiński, M.A. Sentef, Quantum walk versus classical wave: distinguishing ground states of quantum magnets by spacetime dynamics. Phys. Rev. B **102**, 024440 (2020)
16. K. Manouchehri, J. Wang, *Physical Implementation of Quantum Walks* (Springer, Berlin, 2014)
17. H.B. Perets, Y. Lahini, F. Pozzi, M. Sorel, R. Morandotti, Y. Silberberg, Realization of quantum walks with negligible decoherence in waveguide lattices. Phys. Rev. Lett. **100**, 170506 (2008)
18. L. Sansoni, F. Sciarrino, G. Vallone, P. Mataloni, A. Crespi, R. Ramponi, R. Osellame, Two-particle bosonic-fermionic quantum walk via integrated photonics. Phys. Rev. Lett. **108**, 010502 (2012)
19. K.-K. Wang, X.Z. Qiu, L. Xiao, X. Zhan, Z.H. Bian, W. Yi, P. Xue, Simulating dynamic quantum phase transitions in photonic quantum walks. Phys. Rev. Lett. **122**, 020501 (2019)
20. Y. Wang, Z.-W. Cui, Y.-H. Lu, X.-M. Zhang, J. Gao, Y.-J. Chang, M.-H. Yung, X.-M. Jin, Integrated quantum-walk structure and NAND tree on a photonic chip. Phys. Rev. Lett. **125**, 160502 (2020)
21. L. Xiao, T.-S. Deng, K.-K. Wang, Z. Wang, W. Yi, P. Xue, Observation of non-Bloch parity-time symmetry and exceptional points. Phys. Rev. Lett. **126**, 230402 (2021)
22. K.-K. Wang, L. Xiao, J.C. Budich, W. Yi, P. Xue, Simulating exceptional non-Hermitian metals with single-photon interferometry. Phys. Rev. Lett. **127**, 026404 (2021)
23. T. Giordani, E. Polino, S. Emiliani, et al., Experimental engineering of arbitrary qudit states with discrete-time quantum walks. Phys. Rev. Lett. **122**, 020503 (2019)
24. B. Wang, T. Chen, X.-D. Zhang, Experimental observation of topologically protected bound states with vanishing Chern numbers in a two-dimensional quantum walk. Phys. Rev. Lett. **121**, 100501 (2018)
25. C. Chen, X. Ding, J. Qin, Y. He, et al., Observation of topologically protected edge states in a photonic two-dimensional quantum walk. Phys. Rev. Lett. **121**, 100502 (2018)
26. X.-Y. Xu, Q.-Q. Wang, W.-W. Pan, et al., Measuring the winding number in a large-scale chiral quantum walk. Phys. Rev. Lett. **120**, 260501 (2018)
27. X.-Y. Xu, X.-W. Wang, D.-Y. Chen, C.M. Smith, X.-M. Jin, Quantum transport in fractal networks. Nat. Photonics **15**, 703–710 (2021)
28. X.-G. Qiang, Y.-Z. Wang, S.-C. Xue, Implementing graph-theoretic quantum algorithms on a silicon photonic quantum walk processor. Sci. Adv. **7**, eabb8375 (2021)
29. P. Xue, Q. Lin, K. Wang, et al., Self acceleration from spectral geometry in dissipative quantum-walk dynamics. Nat. Commun. **15**, 4381 (2024)
30. M. Monika, F. Nosrati, A. George, et al., Quantum state processing through controllable synthetic temporal photonic lattices. Nat. Photonics **19**, 95–100 (2025). REPORT
31. P. Xue, B.C. Sanders, D. Leibfried, Quantum walk on a line for a trapped ion. Phys. Rev. Lett. **103**, 183602 (2009)
32. R. Matjeschk, C. Schneider, M. Enderlein, et al., Experimental simulation and limitations of quantum walks with trapped ions. New J. Phys. **14**, 035012 (2012)
33. H. Schmitz, R. Matjeschk, C. Schneider, J. Glueckert, M. Enderlein, T. Huber, T. Schaetz, Quantum walk of a trapped ion in phase space. Phys. Rev. Lett. **103**, 090504 (2009)
34. F. Zähringer, G. Kirchmair, R. Gerritsma, E. Solano, R. Blatt, C.F. Roos, Realization of a quantum walk with one and two trapped ions. Phys. Rev. Lett. **104**, 100503 (2010)
35. M. Tamura, T. Mukaiyama, K. Toyoda, Quantum walks of a phonon in trapped ions. Phys. Rev. Lett. **124**, 200501 (2020)
36. T. Chen, C.-X. Huang, B. Gadway, J.P. Covey, Quantum walks and correlated dynamics in an interacting synthetic Rydberg lattice. Phys. Rev. Lett. **133**, 120604 (2024)
37. M. Karski, L. Förster, J.-M. Choi, et al., Quantum walk in position space with single optically trapped atoms. Science **325**, 174 (2009)
38. C. Weitenberg, M. Endres, J.F. Sherson, M. Cheneau, P. Schauß, T. Fukuhara, I. Bloch, S. Kuhr, Single-spin addressing in an atomic Mott insulator. Nature **471**, 319 (2011)
39. T. Fukuhara, P. Schauß, M. Endres, S. Hild, M. Cheneau, I. Bloch, C. Gross, Microscopic observation of magnon bound states and their dynamics. Nature **502**, 76 (2013)
40. D.-X. Xie, T.-S. Deng, T. Xiao, W. Gou, T. Chen, W. Yi, B. Yan, Topological quantum walks in momentum space with a Bose-Einstein condensate. Phys. Rev. Lett. **124**, 050502 (2020)
41. J. Carlström, N. Prokof'ev, B. Svistunov, Quantum walk in degenerate spin environments. Phys. Rev. Lett. **116**, 247202 (2016)
42. A.W. Young, et al., Tweezer-programmable 2D quantum walks in a Hubbard-regime lattice. Science **377**, 885–889 (2022)
43. V.V. Ramasesh, E. Flurin, M. Rudner, I. Siddiqi, N.Y. Yao, Direct probe of topological invariants using Bloch oscillating quantum walks. Phys. Rev. Lett. **118**, 130501 (2017)
44. Z.-G. Yan, Y.-R. Zhang, M. Gong, et al., Strongly correlated quantum walks with a 12-qubit superconducting processor. Science **364**, 753 (2019)
45. M. Gong, S.-Y. Wang, C. Zha, et al., Quantum walks on a programmable two-dimensional 62-qubit superconducting processor. Science **372**, 948 (2021)
46. Y. Wu, W.-S. Bao, S. Cao, et al., Strong quantum computational advantage using a superconducting quantum processor. Phys. Rev. Lett. **127**, 180501 (2021)
47. M. Cheneau, P. Barmettler, D. Poletti, et al., Light-cone-like spreading of correlations in a quantum many-body system. Nature **481**, 484 (2012)
48. J. Zhang, G. Pagano, P.W. Hess, A. Kyprianidis, P. Becker, H. Kaplan, A.V. Gorshkov, Z.-X. Gong, C. Monroe, Observation of a many-body dynamical phase transition with a 53-qubit quantum simulator. Nature **551**, 601 (2017)
49. M.C. Tran, C.-F. Chen, A. Ehrenberg, Hierarchy of linear light cones with long-range interactions. Phys. Rev. X **10**, 031009 (2020)
50. C. Monroe, W.C. Campbell, L.-M. Duan, et al., Programmable quantum simulations of spin systems with trapped ions. Rev. Mod. Phys. **93**, 025001 (2021)
51. T. Zhou, B. Swingle, Operator growth from global out-of-time-order correlators. Nat. Commun. **14**, 3411 (2023)
52. S.-L. Xu, B. Swingle, Scrambling dynamics and out-of-time-ordered correlators in quantum many-body systems. PRX Quantum **5**, 010201 (2024)
53. S.V. Syzranov, A.V. Gorshkov, V. Galitski, Out-of-time-order correlators in finite open systems. Phys. Rev. B **97**, 161114(R) (2018)
54. M. Heyl, F. Pollmann, B. Dóra, Detecting equilibrium and dynamical quantum phase transitions in Ising chains via out-of-time-ordered correlators. Phys. Rev. Lett. **121**, 016801 (2018)
55. M. Gärttner, P. Hauke, A.M. Rey, Relating out-of-time-order correlations to entanglement via multiple-quantum coherences. Phys. Rev. Lett. **120**, 040402 (2018)
56. B. Yoshida, N.Y. Yao, Disentangling scrambling and decoherence via quantum teleportation. Phys. Rev. X **9**, 011006 (2019)
57. C. Murthy, M. Srednicki, Bounds on chaos from the eigenstate thermalization hypothesis. Phys. Rev. Lett. **123**, 230606 (2019)
58. K.A. Landsman, C. Figgatt, T. Schuster, N.M. Linke, B. Yoshida, N.Y. Yao, C. Monroe, Verified quantum information scrambling. Nature **567**, 61 (2019)
59. S. Choi, Y. Bao, X.-L. Qi, E. Altman, Quantum error correction in scrambling dynamics and measurement-induced phase transition. Phys. Rev. Lett. **125**, 030505 (2020)

60. R.J. Lewis-Swan, S.R. Muleady, A.M. Rey, Detecting out-of-time-order correlations via quasiadiabatic echoes as a tool to reveal quantum coherence in equilibrium quantum phase transitions. Phys. Rev. Lett. **125**, 240605 (2020)
61. S.Z. Li, L.-H. Li, S.-L. Zhu, Z. Li, Anderson-Skin dualism (2025). arXiv:2507.05013
62. K.X. Wei, C. Ramanathan, P. Cappellaro, Exploring localization in nuclear spin chains. Phys. Rev. Lett. **120**, 070501 (2018)
63. S.L. Xu, B. Swingle, Locality, quantum fluctuations, and scrambling. Phys. Rev. X **9**, 031048 (2019)
64. M. McGinley, A. Nunnenkamp, J. Knolle, Slow growth of out-of-time-order correlators and entanglement entropy in integrable disordered systems. Phys. Rev. Lett. **122**, 020603 (2019)
65. H.T. Shen, P.F. Zhang, R.H. Fan, H. Zhai, Out-of-time-order correlation at a quantum phase transition. Phys. Rev. B **96**, 054503 (2017)
66. Y. Huang, Y.-L. Zhang, X. Chen, Out-of-time-ordered correlators in many-body localized systems. Ann. Phys. **529**, 1600318 (2016)
67. K. Slagle, Z. Bi, Y.-Z. You, C.K. Xu, Out-of-time-order correlation in marginal many-body localized systems. Phys. Rev. B **95**, 165136 (2017)
68. K. Xu, J.-J. Chen, Y. Zeng, et al., Emulating many-body localization with a superconducting quantum processor. Phys. Rev. Lett. **120**, 050507 (2018)
69. N.Y. Yao, C.R. Laumann, S. Gopalakrishnan, M. Knap, M. Mueller, E.A. Demler, M.D. Lukin, Many-body localization in dipolar systems. Phys. Rev. Lett. **113**, 243002 (2014)
70. H.-Z. Li, X.-J. Yu, J.-X. Zhong, Non-Hermitian Stark many-body localization. Phys. Rev. A **108**, 043301 (2023)
71. C. Li, Spin grouping in ring cavity and its protection on entangled states transfer. Phys. Rev. Lett. **134**, 210803 (2025)
72. E.B. Rozenbaum, S. Ganeshan, V. Galitski, Lyapunov exponent and out-of-time-ordered correlator's growth rate in a chaotic system. Phys. Rev. Lett. **118**, 086801 (2017)
73. I. García-Mata, M. Saraceno, R.A. Jalabert, A.J. Roncaglia, D.A. Wisniacki, Chaos signatures in the short and long time behavior of the out-of-time ordered correlator. Phys. Rev. Lett. **121**, 210601 (2018)
74. B. Yan, L. Cincio, W.H. Zurek, Information scrambling and Loschmidt echo. Phys. Rev. Lett. **124**, 160603 (2020)
75. D.E. Parker, X.Y. Cao, A. Avdoshkin, T. Scaffidi, E. Altman, A universal operator growth hypothesis. Phys. Rev. X **9**, 041017 (2019)
76. T.R. Xu, T. Scaffidi, X.Y. Cao, Does scrambling equal chaos? Phys. Rev. Lett. **124**, 140602 (2020)
77. W.-L. Zhao, Y. Hu, Z. Li, Q. Wang, Super-exponential growth of out-of-time-ordered correlators. Phys. Rev. B **103**, 184311 (2021)
78. D.A. Roberts, D. Stanford, Diagnosing chaos using four-point functions in two-dimensional conformal field theory. Phys. Rev. Lett. **115**, 131603 (2015)
79. J. Maldacena, S.H. Shenker, D. Stanford, A bound on chaos. J. High Energy Phys. **08**, 106 (2016)
80. J. Maldacena, The large-N limit of superconformal field theories and supergravity. Int. J. Theor. Phys. **38**, 1113 (1999)
81. J. de Boer, E. Llabrés, J.F. Pedraza, D. Vegh, Chaotic strings in AdS/CFT. Phys. Rev. Lett. **120**, 201604 (2018)
82. J. Li, R.-H. Fan, H.-Y. Wang, B.-T. Ye, B. Zeng, H. Zhai, X.-H. Peng, J.-F. Du, Measuring out-of-time-order correlators on a nuclear magnetic resonance quantum simulator. Phys. Rev. X **7**, 031011 (2017)
83. M. Gärttner, J.G. Bohnet, A. Safavi-Naini, M.L. Wall, J.J. Bollinger, A.M. Rey, Measuring out-of-time-order correlations and multiple quantum spectra in a trapped-ion quantum magnet. Nat. Phys. **13**, 781 (2017)
84. A. Nahum, S. Vijay, J. Haah, Operator spreading in random unitary circuits. Phys. Rev. X **8**, 021014 (2018)
85. V. Khemani, A. Vishwanath, D.A. Huse, Operator spreading and the emergence of dissipative hydrodynamics under unitary evolution with conservation laws. Phys. Rev. X **8**, 031057 (2018)
86. C.B. Dağ, K. Sun, L.-M. Duan, Detection of quantum phases via out-of-time-order correlators. Phys. Rev. Lett. **123**, 140602 (2019)
87. C.B. Dağ, L.-M. Duan, Detection of out-of-time-order correlators and information scrambling in cold atoms: ladder-XX model. Phys. Rev. A **99**, 052322 (2019)
88. J. Braumüller, A.H. Karamlou, Y. Yanay, et al., Probing quantum information propagation with out-of-time-ordered correlators. Nat. Phys. **18**, 172–178 (2022)
89. S.K. Zhao, Z.-Y. Ge, Z.-C. Xiang, et al., Probing operator spreading via Floquet engineering in a superconducting circuit. Phys. Rev. Lett. **129**, 160602 (2022)
90. Supplementary Materials I, Detailed linear spin wave method, magnon dynamics, otoc and butterfly velocities are provided in S1-S3. S6 provide the comparison of OTOCs between theoretical predictions and the results of Exact diagonalization and Tensor Network method (TDVP)
91. A.M. Childs, J. Goldstone, Spatial search by quantum walk. Phys. Rev. A **70**, 022314 (2004)
92. E.H. Lieb, D.W. Robinson, The finite group velocity of quantum spin systems. Commun. Math. Phys. **28**, 251 (1972)
93. S. Bravyi, M.B. Hastings, F. Verstraete, Lieb-Robinson bounds and the generation of correlations and topological quantum order. Phys. Rev. Lett. **97**, 050401 (2006)
94. J. Jünemann, A. Cadarso, D. Perez-Garcia, A. Bermudez, J.J. Garcia-Ripoll, Lieb-Robinson bounds for spin-boson lattice models and trapped ions. Phys. Rev. Lett. **111**, 230404 (2013)
95. M. Foss-Feig, Z.-X. Gong, C.W. Clark, A.V. Gorshkov, Nearly linear light cones in long-range interacting quantum systems. Phys. Rev. Lett. **114**, 157201 (2015)
96. C.-C. Chien, S. Peotta, M.D. Ventra, Quantum transport in ultracold atoms. Nat. Phys. **11**, 998 (2015)
97. T. Matsuta, T. Koma, S. Nakamura, Improving the Lieb-Robinson bound for long-range interactions. Ann. Henri Poincaré **18**, 519 (2017)
98. T. Kuwahara, K. Saito, Strictly linear light cones in long-range interacting systems of arbitrary dimensions. Phys. Rev. X **10**, 031010 (2020)

Publisher's note